Submitted 5/14/98, To appear in the *Proceedings of the International Conference on Substorms-4*

A CME loop and the January 10, 1997 first substorm

B. T. Tsurutani,[1] J. K. Arballo,[1] G. S. Lakhina,[1] C. M. Ho,[1] J. M. Ajello,[1] J. S. Pickett,[2]
D. A. Gurnett,[2] R. P. Lepping,[3] W. K. Peterson,[4] G. Rostoker,[5] Y. Kamide,[6] and S. Kokubun[6]

Abstract. The January 10, 1997 interplanetary high-speed stream and the resultant first substorm (~0332 to 0334 UT onset) is studied using Wind interplanetary data and Polar UV images, respectively. A 47 minute interval of relatively intense southward interplanetary magnetic field (IMF) (B_S = 4 to 8 nT, where B_S is the southward component of the IMF) bounded by two tangential discontinuities (TDs) is identified sunward of the interplanetary shock and anti-sunward of the magnetic cloud. The TD orientations are used to calculate the solar wind delay times from Wind to the Earth's magnetopause. The estimated arrival times are in excellent agreement with Geotail data (the two discontinuities occurred at 0219 and 0302 UT at Geotail). The IMF B_S event serves primarily to transfer solar wind energy to the magnetosphere/magnetotail, as no substorm expansion phase occurs during the event. The interplanetary B_S event comes after a prolonged northward IMF interval. During the initial part of the B_S event, both polar cap sun-earth aligned arcs formed (part of a theta aurora) and an auroral hot spot along the main arc took place. During this initial interval, an aurora in the shape of a horseshoe developed at a lower (60°) latitude (an oval with a gap in the noon sector). The dawnside portion of the horseshoe aurora became much brighter than the duskside with increasing time. The dawnside polar cap boundary layer (PCBL) broadband waves were well correlated with low energy ion fluxes (H^+, He^{++}, O^+) during the event. It is speculated that this IMF B_S structure may be an outer loop of the CME coming from the sun. Another similar loop is identified just adjacent to the cloud.

Introduction

The purpose of this paper is to study an interplanetary B_S feature ahead of a magnetic cloud and its related auroral and magnetospheric responses. During this IMF B_S event, theta auroras, a midnight hot spot and an eventual asymmetric horseshoe aurora formed. A substorm expansion phase took place after the IMF B_S event had passed. The time sequences of the above, and the various interplanetary, magnetospheric and ionospheric phenomena will be discussed.

Data Analysis

This study utilizes the Wind plasma and magnetic field data, Polar ultraviolet images, plasma wave data, and low energy ion data, and the CANOPUS ground magnetograms. Detailed descriptions of the instruments, instrument modes and sensitivities can be found in: Ogilvie et al. (1995), Lepping et al. (1995), Torr et al. (1995), Gurnett et al. (1995), Shelley et al. (1995), and Rostoker et al. (1995), respectively. The Wind spacecraft was located at a geocentric solar ecliptic (GSE) position (x, y, z) of 86 R_E, -59 R_E, -4 R_E, where R_E is the Earth's radius. This location, calculated discontinuity orientations and the measured solar wind velocities are used to determine the time delays between detection of interplanetary structures at Wind and convection of these structures to the Earth's magnetopause.

The Polar orbit has an ~86° inclination with a ~9 R_E apogee and a ~1.8 R_E perigee, respectively. Since the beginning of the mission, the Polar apogee has been over the northern polar region.

Results

Interplanetary Features

The Wind interplanetary data for the first 6 hours of January 10 are shown in Figure 1. From top-to-bottom are: the interplanetary magnetic field (IMF) plotted in geocentric solar-magnetospheric (GSM) coordinates, the percentage (%) of He^{++}/H^+ density, the He^{++} thermal speed, proton density, proton thermal speed, and solar wind velocity in GSM coordinates. A large magnetosonic pressure wave occurs at ~0053 UT. The onset of the wave is identified by the abrupt increases in plasma density, plasma thermal speed, solar wind velocity and magnetic field strength. The compression of the magnetosphere by the increased ram pressure from the stream led to a faint UV auroral intensification (not shown) which propagated along the auroral oval from noon towards the tail and also from high L to low L. There was no substorm expansion phase caused by this compression, but there were a series of pseudobreakups (to be addressed in a companion paper: Arballo et al., 1998).

Beginning with the shock, the IMF has a long duration northward component. At 0205 UT the IMF turns southward and remains southward until 0252 UT, when the field abruptly turns northward again. The B_S magnitude is initially ~4 nT. It more or less monotonically increases to ~8 nT before the abrupt northward turn. This interval of interest is shaded and the southward IMF interval is crosshatched. It should be noted that there is a slight velocity jump (from 430 to 440 km s^{-1}) at the leading edge of the B_S interval. This event precedes the magnetic cloud event (Burlaga et al., 1998), whose onset is much later at ~ 0459 UT.

Minimum variance analyses have been performed on the discontinuities bounding the B_S event (at the edges of two shaded regions). The maximum, intermediate and minimum eigenvectors are identified by the subscripts 1, 2 and 3, respectively. The discontinuities, plotted in minimum variance coordinates are show in Figure 2. The discontinuity at 0205 UT has a normal direction of (0.88, 0.22, 0.42) in GSE coordinates. The value of the field along the normal direction, normalized by field magnitude, is 0.1. The second discontinuity at 0252 UT has a normal direction of (0.75, 0.43, 0.50) and has a normalized field along the minimum variance direction of 0.01. The λ_1/λ_2 and λ_2/λ_3 eigenvalue ratios

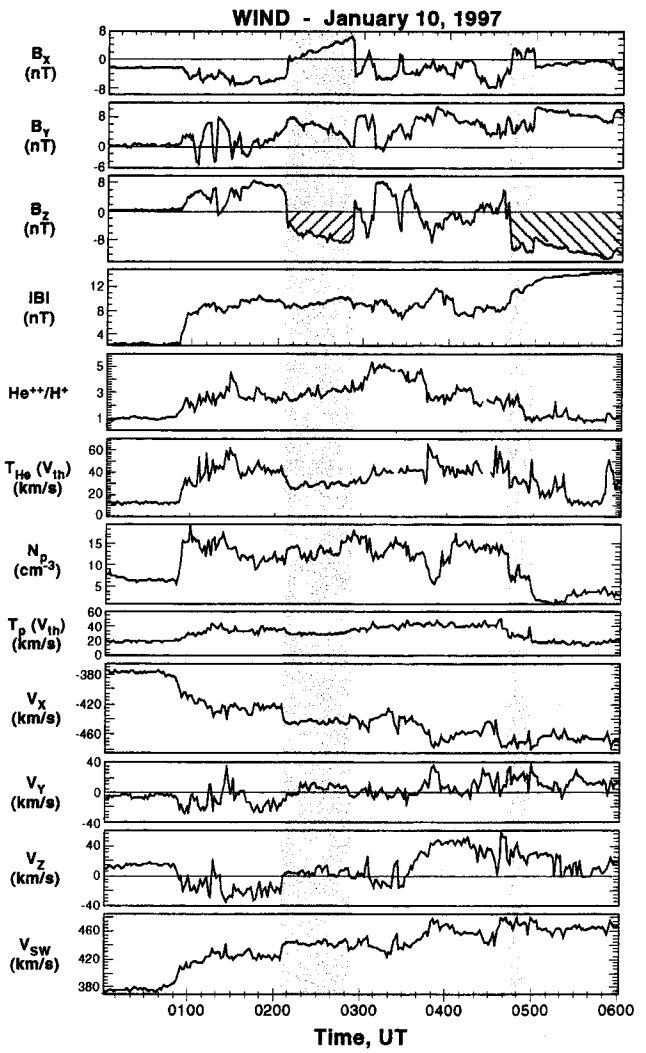

Figure 1. The Wind solar wind magnetic field and plasma data.

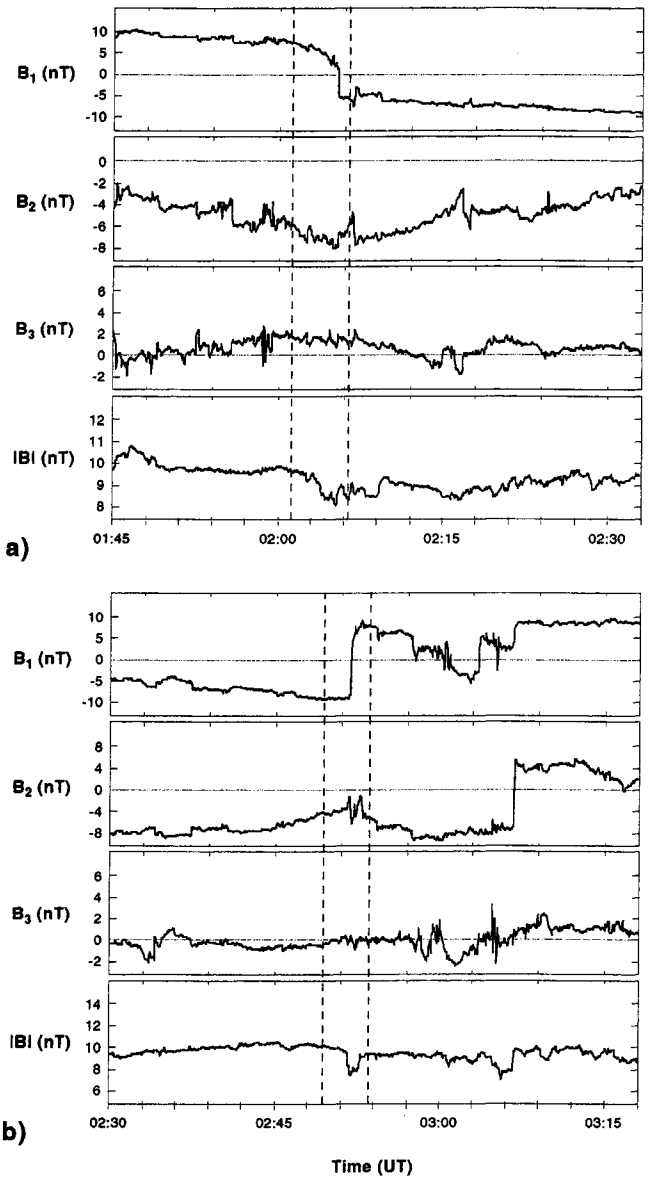

Figure 2. The 0205 UT and 0252 UT discontinuities plotted in minimum variance coordinates. Both events have small normal components, implying that they are tangential in nature.

are 91 and 3.4 respectively for the first discontinuity and 46 and 33 for the second discontinuity. The low field component along the normal directions implies that both discontinuities are most likely tangential (TD) in nature. Tangential discontinuities are believed to be much larger in spatial scale than Alfvén waves and rotational discontinuities (Tsurutani et al., 1990; 1997). The large ratios, λ_2/λ_3 (for the second discontinuity), imply that the discontinuities are well resolved, but the large λ_1/λ_2 values mean the structures are close to being linearly polarized and there might be significant uncertainty in the normal determination. One interpretation of this B_s event is that it is associated with a plasma slab bounded by TDs.

The arrival times of the discontinuities at the Earth's magnetopause are calculated using the spacecraft location, the solar wind convection speeds (430 km s^{-1} and 450 km s^{-1}, respectively) and the discontinuity orientations. The predicted arrival times at the Earth's magnetopause are 0220 UT and 0302 UT. We have also used the Geotail magnetic field measurements as a check for the delay time. This is shown in Figure 3. The Geotail data clearly show the same IMF B_s event. Geotail was in the Earth's magnetosheath at 9.0 R_E, -4.5 R_E, 1.1 R_E and 9.3 R_E, -3.4 R_E, 1.1 R_E, roughly 0.5 R_E upstream of the nominal magnetopause. The discontinuity arrival times at Geotail are 0219 and 0302 UT, almost the same as that predicted from the Wind data/calculations. This excellent agreement supports the idea that this B_s structure is large in scale and is simply convected by the solar wind.

Identification of Two CME Loops

The interplanetary magnetic cloud at 0459 UT is identified by the low proton density (1-2 cm^3), the low temperature (thermal speed V_{th} ~20 km s^{-1}), and the intense magnetic fields (>12 nT). There is, however, a region just prior to the cloud proper which is

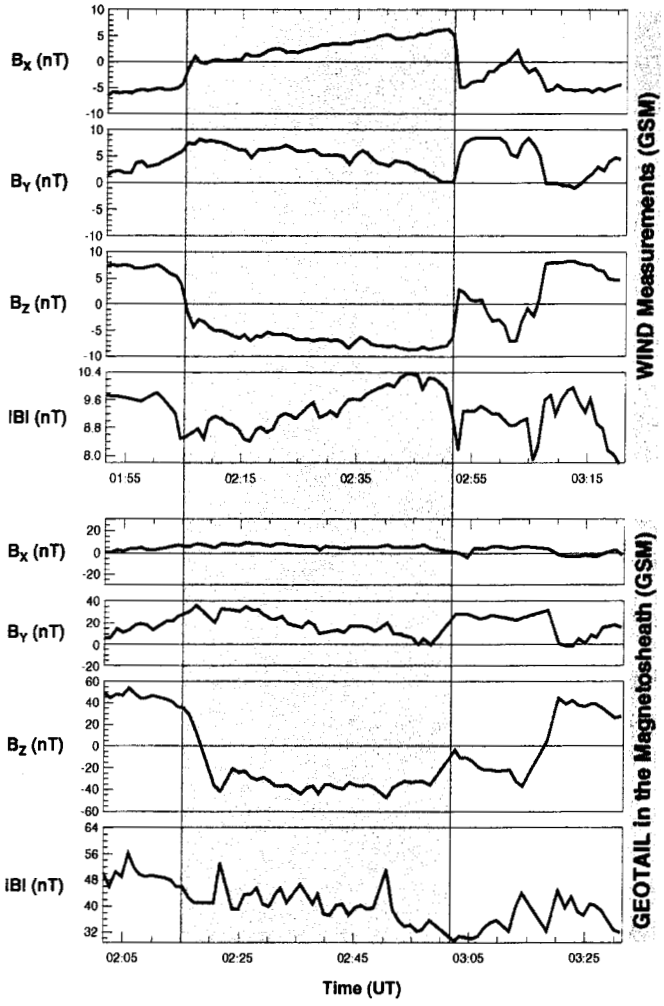

Figure 3. A time-shifted comparison between the Wind and Geotail magnetic field data. Although Geotail is in the magnetosheath, the B_Z structure is quite similar to the structure detected at Wind.

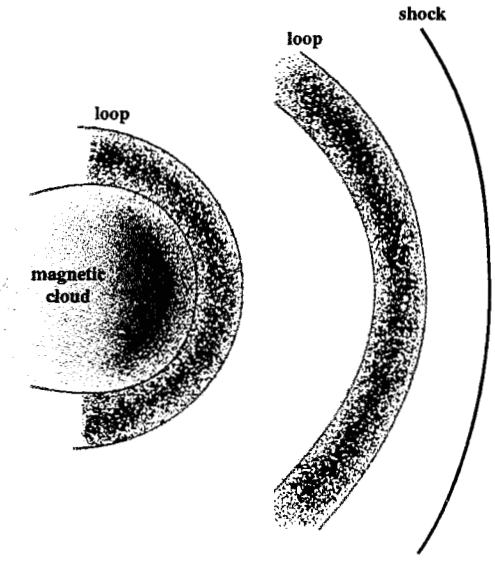

Figure 4. A schematic of the large scale outer loop which leads to the auroral hotspot, the theta aurora, and the horseshoe aurora. It is believed that two such loops have been identified in the Wind magnetic field data.

also of interest. It occurs from 0441 to 0459 UT and it is shaded for emphasis (second shaded region) in Figure 1. The proton density and temperature (thermal speed) are considerably higher than the corresponding values within the magnetic cloud, and they are also lower than the values that occur just prior to the event. The magnetic field magnitude is intermediate between the cloud-proper value and the value slightly earlier in time. This structure looks similar to a "boundary layer".

There is a great deal of similarity between the magnetic field and plasma characteristics in the second shaded region of Figure 1 to that of the event of study (first shaded region). In both regions, $B_X > 0$, $B_Y > 0$ and $B_Z < 0$. The field magnitudes are both ~8-10 nT and the proton thermal velocities ~30 km s^{-1}. The discontinuities at the boundaries of the second region (0441 UT and 0459 UT) have also been studied using minimum variance analyses (not shown). It is found that the normals of these discontinuities are closely aligned with those of the former event. Thus one very interesting possibility is that these two structures are outer loops of the CME (a schematic is shown in Figure 4). If such loops can be identified, and their field orientations are the same as the subsequent magnetic cloud, they could be extremely useful in the prediction of impending magnetic storms.

A case when plasma and fields were similar to magnetic cloud plasma and fields, but was upstream of the cloud, has been reported by Galvin et al. (1987). Recently Tsurutani and Gonzalez (1997) have interpreted regions of this type as magnetic loops preceding the magnetic cloud.

UV Hot Spot, Horshoe Aurora, and Substorm Expansive Phase Onset

The UV aurora corresponding to the time interval of the southward IMF is shown in Figure 5. We show the UV images corresponding to the IMF event and slightly beyond: 0223 UT to 0340 UT. The Lyman-Birge-Hopfield (LBH) long band (~1700 Å) images proceed from top left, across and then down. In each image, noon is at the top.

What is quite remarkable is that the aurora is generally faint throughout the southward B_S interval, with no substorm expansion phase onsets. At the beginning of the IMF B_S interval, there are polar arcs and a very faint auroral oval at high latitudes. There is a "hot spot" at local midnight (0239:10 UT). The hot spot has a size of 2° to 5° and brightens and dims over time (not shown). The relative location is stable. It is originally located where a polar arc "touches" the oval, and it becomes well poleward of the oval as the oval recedes equatorward. The hot spot lasts from prior to 0219 to 0239 UT. During this time period, the IMF B_Y (the dawn-dusk component of the IMF) was positive and decreased with time. These general features of the theta aurora are in good agreement with the model of the theta aurora proposed by Newell and Meng (1995) and Chang et al. (1998).

During the polar arcs and the "hot spot" period, a regularly shaped aurora formed, but at lower latitudes. From 0251 UT onward, a clear "horseshoe-shaped" aurora was present. The UV

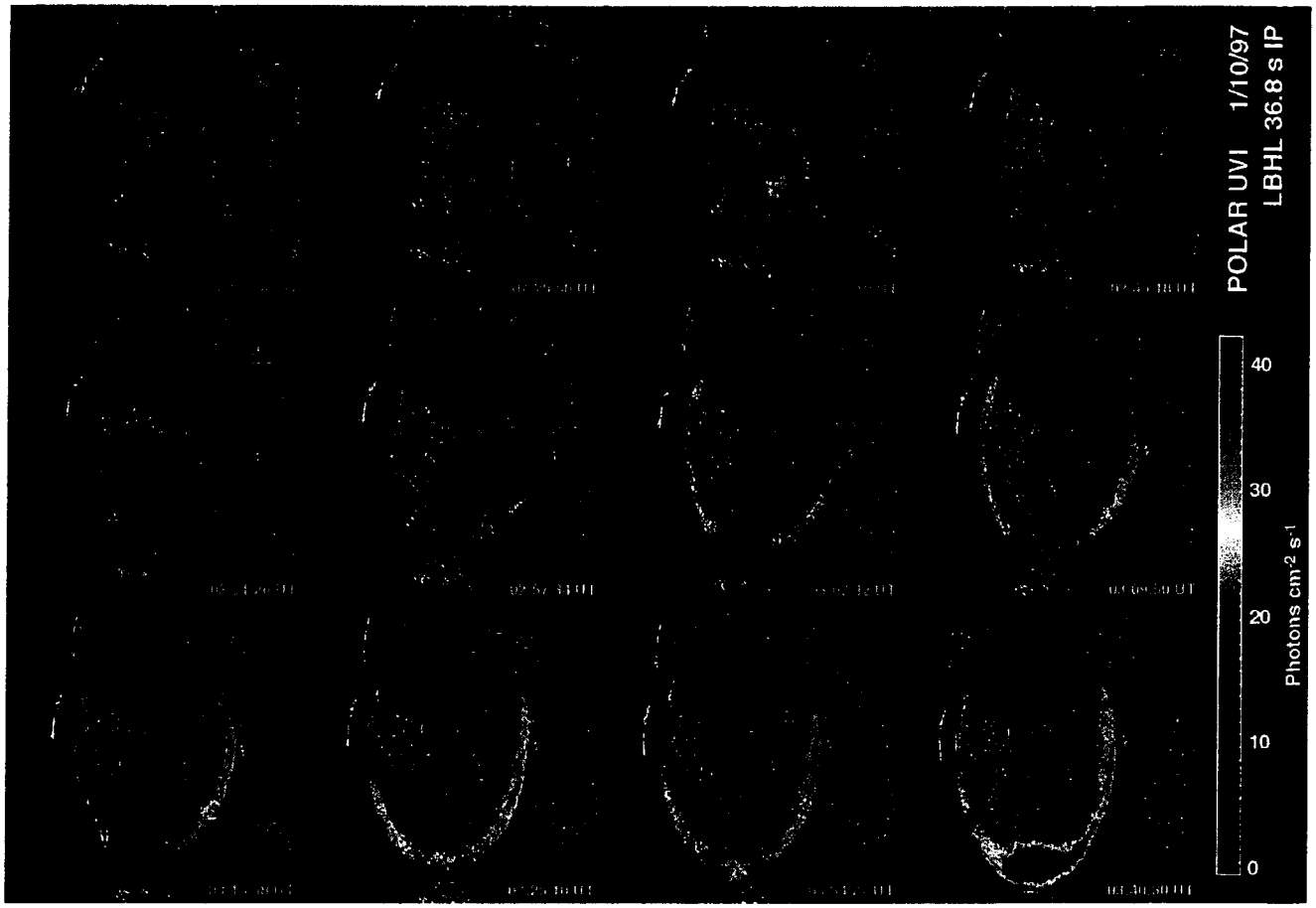

Figure 5. The Polar UV aurora from 0223:50 UT to 0340:30 UT. Local midnight is at the bottom of each panel. Time increases from the upper left to the upper right.

aurora is in the shape of an oval, but with part of the oval missing (a midday "gap" [Dandekar and Pike, 1978] from ~10 to ~14 LT), thus giving the shape of a horseshoe. The auroral intensity is continuous throughout the midnight sector with no particularly remarkable features.

Throughout the 47 minute IMF B_S interval during which the B_S increased from 4 to 8 nT, there was no significant expansive phase activity. This may well be due to the presence of northward IMF fields during the previous hour. The magnetosphere could have been brought to a low level "ground state" by the northward field.

From 0312 UT until 0334 UT, the horseshoe aurora becomes asymmetric in brightness, with the dawnside aurora becoming far brighter than the duskside. This brightening on the dawnside increases with time. High latitude magnetometer data (not shown here) indicate that a weak westward electrojet (~-300 nT) was peaked at ~530 MLT, coinciding with the peak in the dawnside luminosity.

At 0334 UT, the first hint of a substorm expansion phase onset is noted by a small hot spot at local midnight within the auroral oval. This onset time is uncertain within ~-2 min., due to the ~3-min. cadence of the LBH-Long filter imaging. The Greenland magnetometer identified the onset at essentially the same time, and its maximum intensity was only ~-200 nT. The "hot spot" is indeed a spot on this scale and is not elongated in the east-west direction. In subsequent images, the auroral substorm becomes fully developed (see 0340 UT).

IMF B_N Turning as Substorm Expansive Phase Trigger?

The sharp northward IMF turning occurred at 0302 UT at Geotail. A second B_N turning occurred 15 min. later. The substorm onset time was 0334 UT. Thus the delay for the first B_N turning would be ~30-32 min., and ~15-17 min. for the second B_N turning. Lyons et al. (1997) have determined that the delay between IMF B_N triggers at the magnetopause and substorm onsets is ~ 9 ± 4.5 min.

Concerning the local midnight hot spot existing from 0224 to 0239 UT, there were some small IMF B_N turnings of magnitude of 1-2 nT in the corresponding Wind IMF data at the corresponding times. However, it should be noted that the general trend was for B_S to increase from 4 nT to 8 nT over the IMF B_S interval.

PCBL Wave-Particle Interactions

There have been scientific arguments that low latitude boundary layer (LLBL) waves can cause the quiet time dayside aurora (Tsurutani et al., 1981). The question here is do they cause the

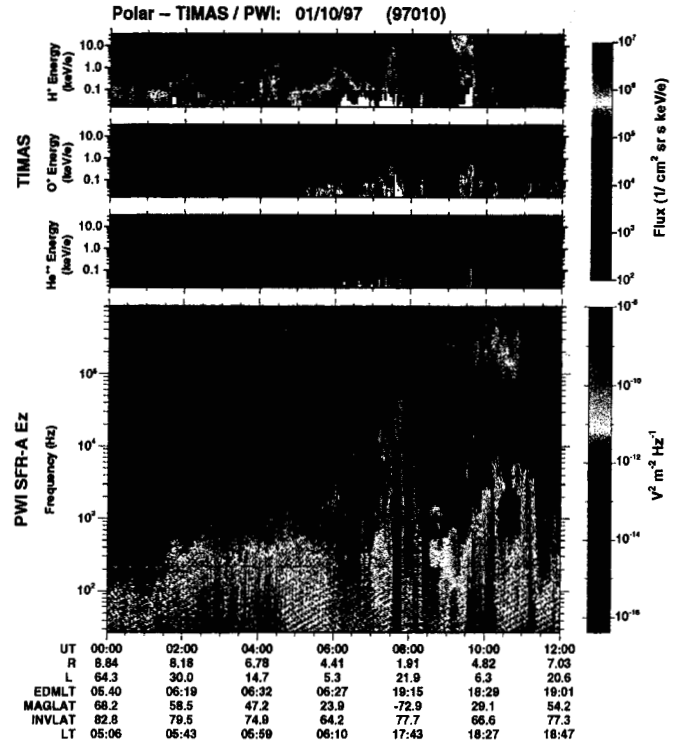

Figure 6. Polar wave and particle correlations. The first 3 panels show the Polar TIMAS ions (H^+, O^+, and He^{++}) fluxes. The bottom panel shows the Polar PWI plasma wave data. At the bottom of the figures various orbit parameters are presented in the tabular form, namely, universal time (UT), radial distance from the center of the Earth (R_E), L value, eccentric dipole magnetic local time (EDMLT), magnetic latitude (MAGLAT), invariant latitude (INVLAT), and local time (LT) are shown.

horseshoe aurora and can they explain the dayside brightening, e.g., are the waves more intense on the dawnside than on the duskside? We unfortunately do not have a continuous monitor of these waves because the measurements are in situ spacecraft measurements. It has been speculated (Pickett et al., 1997; Ho et al., 1997; Tsurutani et al., 1998) that the polar cap boundary layer (PCBL) waves are on the same field lines as the LLBL waves, and can perhaps be used as a proxy to what is occurring at higher altitudes. The Polar plasma wave sweep frequency receiver (SFR) data is given in Figure 6 (bottom panel). The intensity color code is given at the right. The spacecraft was in a dawn-dusk trajectory. At the time of the IMF B_S event, the spacecraft was at local dawn (~6.3 MLT) at a distance of ~7.5 R_E. At this time, the broadband plasma waves having frequencies from 26 Hz to a few times 10^3 Hz were relatively weak compared to other intervals previously examined (Tsurutani et al., 1998). A more typical example of PCBL waves is found at 1110-1120 UT on the duskside, for contrast. The waves are usually short in duration and have intensities $>10^{-9}$ $(V/m)^2/Hz$. There is similarly no remarkable wave feature noticeable between 0310 to 0334 UT when the horseshoe aurora develops and the dawn-dusk auroral brightness asymmetry becomes apparent. There is also no remarkable wave feature (or dawnside auroral features) during substorm onset in the 0334 UT image.

The first unusual wave signature is found from 0735 to 0750 UT during the perigee pass over the southern auroral zones. By this time, the magnetic storm is well developed and there is a distinct dawn (0735-0750 UT) and dusk (0810 - 0820 UT) asymmetry. However, the UV auroral viewing geometry is poor at that time and we unfortunately cannot comment on the dawn and dusk auroral features in any detail.

The intensity and distribution of the field-aligned currents have been examined using over 57 northern auroral zone magnetometer stations (not shown). We find that the dawnside currents are significantly more intense than duskside currents at this time, similar to the UV imaging results.

Conclusions

We have demonstrated that a IMF B_S event, which had a long duration (47 minutes) intense southward B_Z field (B_S = 4 to 8 nT), only led to the development of a horseshoe-shaped aurora with no substorm expansion phases. It is noted that a long period (~1 hour) northward IMF interval preceded the IMF B_S event. Thus, one interpretation for the lack of a substorm expansive phase onset during the B_S event passage is that the prior IMF B_N interval led to the lowering of energy storage in the magnetospheric/magnetotail system. The end of the 47 min. interval of IMF B_S was abruptly terminated by a northward turning. The substorm expansive phase onset occurred well after this B_N turning.

During the initial portion of the IMF B_S interval, there were auroral forms near local midnight spanning ~67° to 60° latitude. There were also transpolar arcs (theta aurora) extended poleward of this midnight region. It should be noted that these theta auroras occurred during an IMF B_S event (not during northward IMFs) in agreement with Newell and Meng (1995).

A small scale (2° to 5°) hot spot formed along one of the main transpolar arcs at midnight where the arc coincided with the auroral oval. The hot spot was relatively stable in location, but brightened and dimmed over time. It lasted over 15 min. and disappeared when the polar arcs faded.

During the late portion of the IMF B_S interval, formation of a stable, low altitude (60°) horseshoe shaped auroral occurred. During this interval, precipitation in the polar regions all but disappeared. It should be noted that the horseshoe aurora is considerably different in shape and interplanetary IMF dependence than "horsecollar" auroras (Hones et al., 1989, Cumnock et al., 1997).

The low intensity of the PCBL waves at the time of the asymmetric horseshoe aurora was also a surprise. Polar passed through the dawn region where the aurora was most intense. These waves are well correlated with the energetic ion fluxes as seen from Figure 6. Preliminary analyses of the angle-time distributions of He^{++} and H^+ for the interval (0000 - 1200) UT indicate that Polar was intermittently seeing the boundary layer plasma from ~ 0140 to ~ 0420 UT. Probably the reconfigurations of the large scale convection patterns in response to changing north-south component of the IMF (Maynard et al., 1998) are responsible for removing the most intense boundary layer plasma away from Polar, thus resulting in the low level of PCBL waves.

The IMF B_S interval feature was shown to be very similar to those of a "boundary region" just adjacent to the magnetic cloud.

These two regions have been identified as loops of a CME. The magnetic cloud is the "dark region" of the CME. It is noted that the IMF B_Z direction of the loops and the magnetic cloud are the same. Thus, if this feature is the same for other CMEs, loop identification could be extremely useful in the prediction of impending magnetic storms.

Acknowledgments. Portions of this work were performed at the Jet Propulsion Laboratory, California Institute of Technology, Pasadena, under contract with the National Aeronautics and Space Administration. We wish to thank the Polar project which funded the UVI and PWI data analyses presented in this paper. The work of GR was supported by the National Science and Engineering Research Council of Canada. CANOPUS was constructed and is operated by the Canadian Space Agency. GSL would like to thank the National Research Council for the award of a Senior Resident Research Associateship at Jet Propulsion Laboratory. We wish to thank A. Lazarus and J. Steinberg for valuable discussions concerning the interpretation of the Wind data.

References

Arballo, J.K., B.T. Tsurutani, X.-Y. Zhou, et al., Pseudobreakups during January 10, 1997, *Proceedings of the International Conference on Substorms-4*, 1998.

Burlaga, L., R. Fitzenreiter, R. Lepping, et al., A magnetic cloud containing prominence material: January, 1997, *J. Geophys. Res.*, in press, 1998.

Chang, S.-W., J. D. Scudder, J.B. Sigwarth, et al., A comparison of a model for the theta aurora with observations from Polar, Wind, and Super Darn, *J. Geophys. Res.*, in press, 1998.

Cumnock, J.A., J.R. Sharber, R.A. Heelis, et al., Evolution of the global aurora during positive B_Z and varying IMF B_Y conditions, *J. Geophys. Res., 102*, 17489, 1997.

Dandekar, B.S. and C.P. Pike, The midday, discrete auroral gap, *J. Geophys. Res., 83*, 4227, 1978.

Galvin, A.B., F.M. Ipavich, G. Gloeckler, et al., Solar wind ion charge status preceding a driver plasma, *J. Geophys. Res., 92*, 12069, 1987.

Gurnett, D.A., A.M. Persoon, R.F. Randall, et al., The POLAR plasma wave instrument, in *The Global Geospace Mission*, ed. by C.T. Russell, Kluwer, 597, 1995.

Ho, C.M., B.T. Tsurutani, A. Boonsiriseth, et al., Wideband plasma waves in the polar cap boundary layer: POLAR observations, *Proceedings of the third SOLTIP symposium*, Beijing, China, ed. by M. Dryer, in press, 1998.

Hones, E.W., Jr., J.D. Craven, L.A. Frank, et al., The horse-collar aurora: A frequency pattern of the aurora in quiet times, *Geophys. Res. Lett., 16*, 37, 1989.

Lepping, R.P., M.H. Acuna, L.F. Burlaga, et al., The WIND magnetic field investigation, in *The Global Geospace Mission*, ed. by C. T. Russell, 207, 1995.

Lyons, L.R., G.T. Blanchard, J.C. Samson, et al., Coordinated observations demonstrating external multistorm triggering, *J. Geophys. Res., 102*, 27039, 1997.

Maynard, N.C., W.J. Burke, D.R. Weimer, et al., POLAR observations of convection with northward IMF at dayside high latitudes, *J. Geophys. Res., 103*, 29, 1998.

Ogilvie, K.W., D.J. Chorney, R.J. Fitzenreiter, et al., in *The Global Geospace Mission*, ed. C.T. Russell, Kluwer, 55, 1995.

Newell, P.T. and C.-I. Meng, Creation of theta auroras: The isolation of plasma sheet fragments in the polar cap, *Science, 270*, 1338, 1995.

Pickett, J.S., R.R. Anderson, L.A. Frank, et al., Correlative magnetopause boundary layer observations, *EOS, 78*, S291, 1997.

Rostoker, G., J.C. Samson, F. Creutzberg, et al., CANOPUS - A ground based instrument array for remote sensing the high latitude ionosphere during the ISTP/GGS program, in *The Global Geospace Mission*, ed. by C.T. Russell, Kluwer, 743, 1995.

Shelley, E.G., A.G. Ghielmetti, H. Balsiger, et al., The toroidal imaging mass-angle spectrometer (TIMAS) for the POLAR mission, *Space Science Rev., 71*, 497, 1995.

Torr, M.R., D.G. Torr, M. Zukic, et al., A far ultraviolet imager for the International Solar-Terrestrial Physics mission, in *The Global Geospace Mission*, ed. by C.T. Russell, Kluwer, 329, 1995.

Tsurutani, B.T., E.J. Smith, R.M. Thorne, et al., Wave-particle interactions at the magnetopause: Contributions to the dayside aurora, *Geophys. Res. Lett., 8*, 183, 1981.

Tsurutani, B.T., T. Gould, B.E. Goldstein, et al., Interplanetary Alfvén waves and auroral (substorm) activity: IMP-8, *J. Geophys. Res., 95*, 2241, 1990.

Tsurutani, B.T., K.-H. Glassmeier, and F.M. Neubauer, A review of nonlinear low frequency (LF) wave observations in space plasmas: On the development of plasma turbulence, in *Nonlinear Waves and Chaos in Space Plasma*, ed. by T. Hada and H. Matsumoto, Terra Sci. Publ., Tokyo, 1, 1997.

Tsurutani, B.T. and W.D. Gonzalez, The interplanetary causes of magnetic storms: A review, in *Magnetic Storms*, ed. by B.T. Tsurutani, W.D. Gonzalez, Y. Kamide and J.K. Arballo, Am. Geophys. Un., Geophys. Monograph *98*, 77, 1997.

Tsurutani, B.T., G.S. Lakhina, C.M. Ho, et al., Broadband plasma waves observed in the polar cap boundary layer (PCBL): Polar, in press, *J. Geophys. Res.*, 1998.

J. M. Ajello, J. K. Arballo, C. M. Ho, G. S. Lakhina, B. T. Tsurutani, Jet Propulsion Laboratory, California Institute of Technology, Pasadena, California 91109 (e-mail: Bruce.Tsurutani@jpl.nasa.gov).

D. A. Gurnett and J. S. Pickett, Department of Physics and Astronomy, 203 Van Allen Hall, University of Iowa, Iowa City, Iowa 52242-1479.

R. P. Lepping, Code 695.0, Goddard Space Flight Center, Greenbelt, Maryland.

W. K. Peterson, Lockheed Space Science Laboratory, Palo Alto, California.

G. Rostoker, Department of Physics, University of Alberta, Edmonton, Alberta, Canada.

Y. Kamide and S. Kokubun, Solar-Terrestrial Environment Laboratory, Nagoya University, Honohara 3-13, Toyokawa, Aichi-ken 442, Japan.

[1]Jet Propulsion Laboratory, California Institute of Technology, Pasadena.

[2]Department of Physics and Astronomy, University of Iowa, Iowa City.

[3]Goddard Space Flight Center, Greenbelt, Maryland.

[4]Lockheed Space Science Laboratory, Palo Alto, California.

[5]Department of Physics, University of Alberta, Edmonton, Alberta, Canada.

[6]Solar-Terrestrial Environment Laboratory, Nagoya University, Toyokawa, Aichi-ken, Japan.